



Baicalein attenuates caspase-independent cells death via inhibiting PARP-1 activation and AIF nuclear translocation in cerebral ischemia/reperfusion rats

Wei-Han Li^{1,2} · Ying-Lin Yang^{1,2} · Xiao Cheng^{1,2} · Man Liu² · Shan-Shan Zhang² · Yue-Hua Wang^{1,2} · Guan-Hua Du^{1,2}

Published online: 27 April 2020

© Springer Science+Business Media, LLC, part of Springer Nature 2020

Abstract

It is reported that baicalein can activate PI3K/AKT pathway, inhibit caspase activation and reduce cerebral infarct volume in middle cerebral artery occlusion (MCAO) rats. However, a caspase-independent mechanism initiated by poly (ADP-ribose) polymerase-1 (PARP-1) activation has been reported to make more contribution to cells death after ischemic stroke. In the present study, we established a cerebral ischemia/reperfusion (I/R) rat model through middle cerebral artery occlusion following reperfusion to investigate the mechanisms of ischemic tissue recovery following baicalein treatment. The data showed that baicalein treatment at dose of 100 mg/kg for 7 days significantly inhibited the release of cytokines, activation of PARP-1, nuclear translocation of apoptosis-inducing factor (AIF) and macrophage migration inhibitory factor (MIF) in cerebral I/R rats, therefore decreased cerebral infarct volume and neurological scores. Then, we further investigated the signal transduction mechanisms of ischemic tissue protection by baicalein *in vitro*. Following oxygen and glucose deprivation (OGD) in SH-SY5Y cells, the mitochondrial AIF was translocated into nucleus after 12 h. The co-immunoprecipitation analysis showed that the interaction between AIF and MIF was activated by OGD and subsequently resulted in MIF nuclear translocation. Also, the baicalein inhibited apoptosis, reduced oxidative stress, protected mitochondrial function and restored mitochondrial membrane potential in OGD cells. The results obtained from both *in vivo* and *in vitro* study demonstrated the PARP-1/AIF pathway involved in mechanisms of baicalein to protect the cerebral tissues from ischemic injury.

Keywords Programed cells death · PARP-1 activation · AIF nuclear translocation · Parthanatos

Abbreviations

MCAO	Middle cerebral artery occlusion.	tPA	Tissue plasminogen activator.
PARP-1	Poly (ADP-ribose) polymerase-1.	TTC	Triphenyl tetrazolium chloride.
I/R	Ischemia/reperfusion.	ROS	Reactive oxygen species.
AIF	Apoptosis-inducing factor.	CCA	Common carotid artery.
MIF	Macrophage migration inhibitory factor.	ECA	External carotid artery.
OGD	Oxygen and glucose deprivation.	ICA	Internal carotid artery.
		MCA	Middle cerebral artery.
		MRI	Magnetic resonance imaging.
		CO-IP	Co-immunoprecipitation.
		PFA	Paraformaldehyde.
		CMC-Na	Sodium carboxymethylcellulose.
		LDF	Laser doppler flowmetry.

✉ Yue-Hua Wang
wangyuehua@pku.org.cn

✉ Guan-Hua Du
dugh@imm.ac.cn

¹ State Key Laboratory of Bioactive Substance and Function of Natural Medicines, Institute of Materia Medica, Chinese Academy of Medical Sciences & Peking Union Medical College, Beijing 100050, China

² Beijing Key Laboratory of Drug Target Identification and New Drug Screening Institute of Materia Medica, Chinese Academy of Medical Sciences & Peking Union Medical College, Beijing 100050, China

Introduction

With the advanced medical treatment, the death rates of ischemic stroke have been significantly decreased in the recent years [1, 2]. Especially, the injection with tissue plasminogen activator (tPA) can quickly restore blood

flow to the brain to improve the chances of survival and reduce complications in patients [3]. However, there is a potential risk of tPA to cause hemorrhaging when used in clinical [4–6]. More drugs need to be discovered to effectively treat the stroke patients.

Many studies have been reported to investigate the mechanisms of neuronal damage occurring in stroke patients in order to develop new drugs [7, 8]. For example, it is reported that the cerebral I/R can activate various types of cell death including apoptosis, necrosis and necroptosis [9, 10]. Necrosis, known as accidental cell death, is characterized to be the uncontrolled death dominating in ischemic core. Apoptosis, known as programmed cell death, prevails in the penumbra after cerebral I/R. The regulation of apoptosis in the penumbra attracts more attention in stroke treatment because of its restorability.

The caspase-mediated cells death has been identified as the key event for brain damage during cerebral I/R [11]. Recently, many new types of caspase-independent mechanisms were reported to involve in cells death of stroke [12–14]. Among them, the poly (ADP-ribose) polymers initiate cell death called parthanatos has been found to play an important role during the cerebral I/R [15–17]. In parthanatos, mitochondria were key factor to determine the cell death [18]. It worked as a main source of ROS production and kept the balance between oxidation and antioxidation during the normal condition [19]. However, cerebral I/R broke the balance, caused accumulation of ROS and followed by DNA damage, PARP-1 activation and mitochondrial AIF translocation into the nucleus [20–22]. Ultimately, the large-scale DNA fragmentation and late caspase activation led to dysfunction of mitochondria, failing to generate ATP and ended up with cell collapse [18].

Baicalein (5,6,7-trihydroxyflavone) is a natural flavonoid subtracted from the roots of *Scutellaria baicalensis* Georgi. The increasing evidences showed its neuroprotective effects on stroke, which were related to its anti-inflammation, anti-oxidation and protection of mitochondrial function [23–26]. However, the effects of baicalein treatment on parthanatos after cerebral I/R have not been reported. In this study, we have investigated the effects of baicalein treatment on this new type of cells death in OGD cells and MCAO rat model. To further elucidate its mechanisms to reduce cerebral ischemic injury, the signal activation of PARP-1 and AIF/MIF translocation were also investigated.

Results

Baicalein reduced cerebral infarction, edema and neurological scores after cerebral I/R

The cerebral infarction and edema images using triphenyl tetrazolium chloride (TTC) staining and magnetic resonance imaging (MRI) scanning were presented in Fig. 1a, d. There was no cerebral infarction and edema observed in rats of sham group. From the MRI data in Fig. 1e, f, ischemic injury induced a mean infarct volume of 34.7% on day 4 and 30% on day 7 in I/R group. And the infarct volume was reduced by 7.2% on day 4 and 11.1% on day 7 following 100 mg/kg baicalein treatment. Similarly, the mean edema rate was 8.1% on day 4 and 3.7% on day 7 in I/R group. And the edema rate was reduced by 4.6% on day 4 and 0.8% on day 7 in baicalein treatment group. Besides, no neurological function loss (score 0) was found in rats in sham group. Compared with the corresponding vehicle treated I/R group, the mean neurological score was reduced from 2.4 to 1.4 on day 7 after baicalein treatment. Besides, the TTC staining showed a consistent result with MRI as shown in Fig. 1a, b.

Baicalein inhibited cytokines production in ischemic tissues after cerebral I/R

To evaluate the effects of baicalein treatment on cytokine production in ischemic brain tissues, a Cytokine Array Q67 (RayBiotech) of total 67 cytokines were measured in the ischemic cerebral tissues after MCAO. The expression of 9 cytokines including MCP-1, Decorin, TIMP-1, ICAM, Neuropilin-1, Gas1, P-Cadherin, Galectin-1 and Notch-2 in the ischemic group animals were significantly elevated at day 7 compared to the sham group. After baicalein treatment, significant reductions of these cytokines were measured as shown in Fig. 2.

Baicalein inhibited the expression of cytochrome C in ischemic cerebral cortex after cerebral I/R

The increasing expression of cytochrome C is considered one of the hallmarks of apoptosis. We performed immunofluorescence staining to assess the effects of baicalein on expression of cytochrome C in the ischemic brain tissues on day 7 in each rat. As shown in Fig. 3b, the fluorescence intensity of cytochrome C in cerebral cortex in I/R group was 2.05 folds compared with sham group. After baicalein treatment, the fluorescence intensity of cytochrome C was significantly reduced by 40.5%.

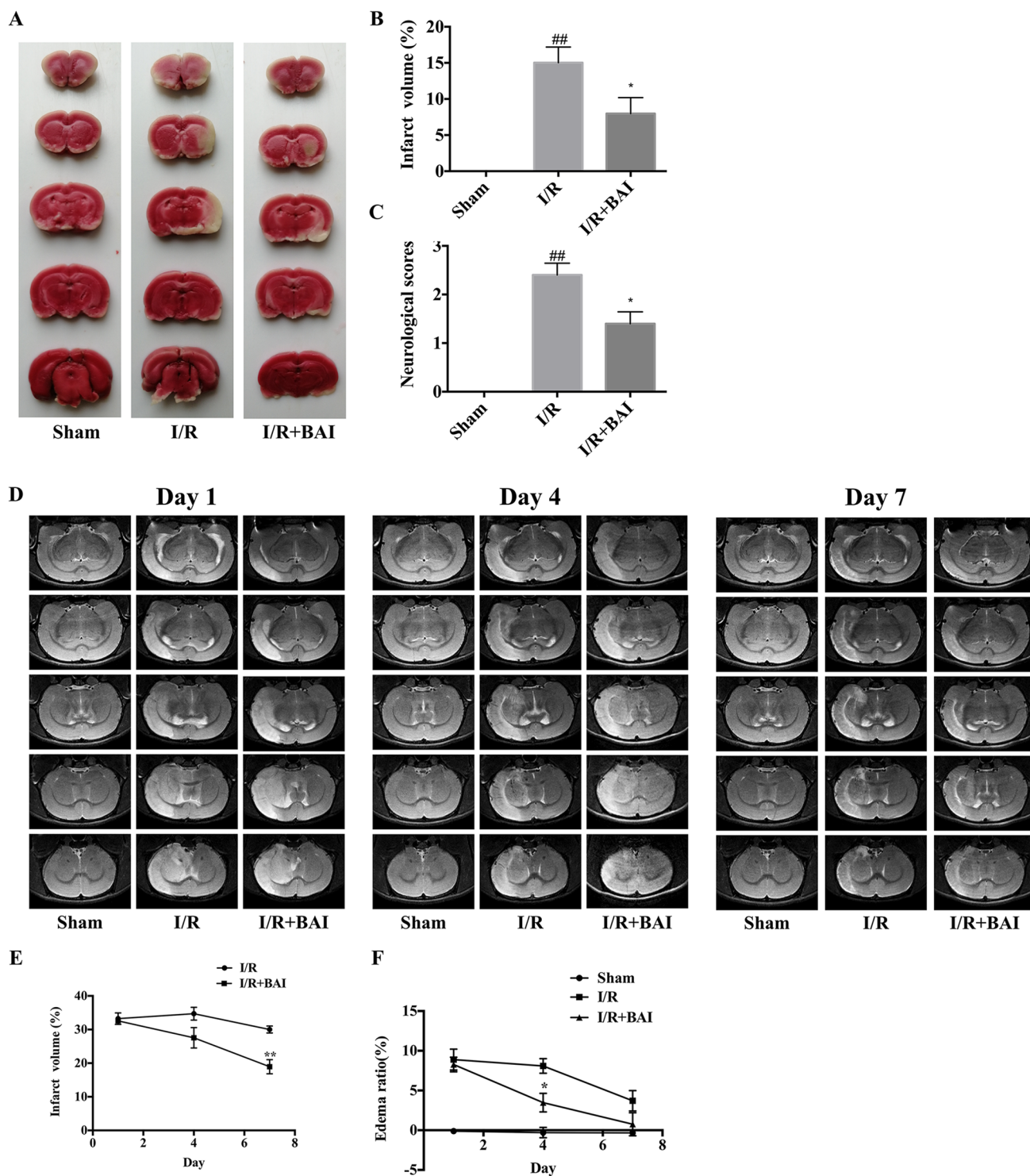


Fig. 1 Effects of baicalein on cerebral infarction, edema and neurological score in cerebral I/R rats. **a** Representative images of cerebral infarction following TTC staining. **b** Statistical analysis on infarct volume on day 7 by TTC staining (n=05 in each group). **c** Statistical analysis on neurological scores of rats on day 7 (n=05 in each group). **d** Representative MRI images of cerebral infarction and

edema. **e** Comparison of infarct volume from MRI examination on day 1, 4, 7 of each group in rats (n=03 in each group). **f** Comparison of cerebral edema ratio from MRI examination on day 1, 4, 7 of each group in rats (n=03 in each group). Data were presented as mean±SEM. ^{##} p<0.01 vs. sham group; ^{*}p<0.05 vs. I/R group

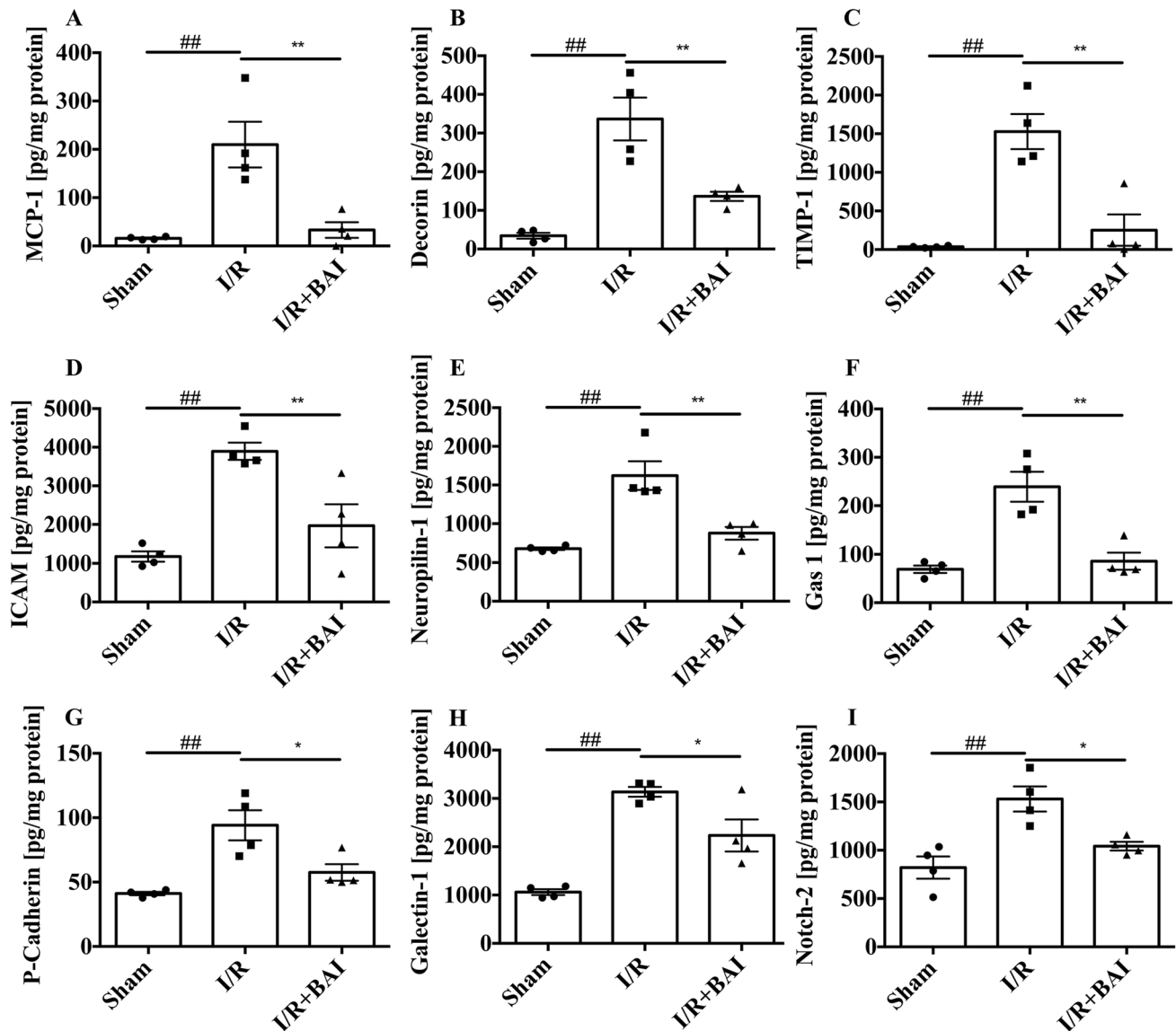


Fig. 2 Cytokines profile measured by protein Array in ischemic cortices of sham control, cerebral I/R and baicalein treatment animals. The concentrations of cytokines were shown as pg/mg protein. Data

were presented as mean \pm SEM ($n=04$ in each group). # $p<0.05$, ## $p<0.01$ vs. sham group; * $p<0.05$, ** $p<0.01$ vs. I/R group

Baicalein inhibited the expression of PARP-1, reduced the nuclear translocation of MIF and AIF in ischemic tissues after cerebral I/R

The PARP-1 activation was the initiation of pathanatos. The expression of PARP-1 was measured using Western blot analysis, the data showed the relative expression of this DNA repairing enzyme was increased by 1.47 folds in cerebral I/R rats as compared to sham group. However, the PARP-1 levels were significantly reduced in baicalein treatment group. The AIF and MIF nuclear translocation followed PARP-1 activation, so we measured the amount of MIF and AIF protein in nuclear and cytoplasmic fraction. The Western blot analysis results

showed that higher amounts of MIF and AIF were located in nucleus after cerebral I/R. After baicalein treatment, the amounts of MIF and AIF in nuclear fraction were decreased. However, in the cytoplasm, the amounts of MIF and AIF were same in each group as shown in Fig. 3g, h. These data suggested that inhibition of PARP-1 and MIF/AIF signal pathways was involved in the protection of ischemic injury of brain tissue following baicalein treatment.

Baicalein improved cellular viability and mitochondrial function in OGD treated cells

In the *in vitro* study, we firstly examined the cytotoxicity of baicalein on human neuronal SH-SY5Y cells. The cells were treated with baicalein at the dose of 1, 5, 10, 15 and 20 μM for 12 h. Then the cell viability was determined by CCK8 assay. The data showed that baicalein had no cytotoxic effects on SH-SY5Y cells at the dose of 1–20 μM . To determine the protective effects of baicalein on SH-SY5Y cells after OGD, the cells were exposed to OGD and different doses of baicalein simultaneously for 12 h. As shown in Fig. 4b, the exposure to OGD caused cytotoxicity as compared with control group cells. Following baicalein treatment, the cell viability was significantly increased at the dose of 5 and 10 μM .

Since the ROS accumulation and ATP consuming played a role in mitochondrial dysfunction after OGD, we measured the amounts of ROS and ATP in the cells of each group. The amounts of ROS production were indicated by the intensity of DCF fluorescence staining in Fig. 4d. The data showed that OGD caused depletion of ATP production. The baicalein treatment increased the ATP levels in a dose dependent manner from 1 to 15 μM as shown in Fig. 4c.

The effects of baicalein treatment on cell apoptosis and necrosis were investigated after OGD. The ratio of apoptotic and necrotic cells was quantified by Annexin V binding and PI uptake using flow cytometry analysis. Annexin V was used to detect the exposure of phosphatidyl serine in apoptotic cells and co-stained with PI to mark the necrotic cells [27]. Therefore, Annexin V was used with PI to distinguish cells at different apoptosis stages. The data showed the ratio of Annexin V+/PI+ cells was increased in OGD group and significantly decreased at 5 μM baicalein treatment, which indicated the protection of baicalein treatment on cells from occurring apoptosis and necrosis after OGD.

Baicalein restored mitochondrial membrane potential in OGD treated cells

Based on the protection results of baicalein from cell injury after OGD as shown above, a dose of 5 μM baicalein was selected to investigate its effects on mitochondrial membrane potential in cells after OGD. As shown in Fig. 5, the normal mitochondria can be stained by Mito-Track CMXRos as red and the nucleus were stained by Hoechst 33342 as blue through fluorescence staining. When oxidative stress and apoptosis occur, mitochondrial membrane potential is decreased and the intensity of red fluorescence will be reduced. The data in Fig. 5a showed the reduced fluorescence staining on the cellular mitochondria membrane potential following OGD. After treatment with 5 μM baicalein, the mitochondrial membrane potential was significantly

increased compared to OGD treatment group. This data suggested that the protective effects on OGD cells following baicalein treatment may be mediated by the recovery of mitochondrial membrane potential to prevent the cells from apoptosis and oxidative stress.

Baicalein inhibited mitochondrial AIF translocation into the nucleus in OGD treated cells

To investigate translocation of AIF in OGD cells following baicalein treatment, the mitochondrial and nuclear protein were isolated and the Western blot was performed to detect the expression of AIF in each fraction. In OGD group cells, the levels of AIF in nuclear fraction were much higher than those of control group. After baicalein treatment, the amounts of AIF inside the nuclear were significantly reduced. This suggested that baicalein can inhibit the translocation of AIF from cytoplasm into nuclear, which might reduce the signal activation and prevent the cells from injury after OGD. Interestingly, we also found that the amounts of AIF protein in mitochondrial were increased in OGD group. However, baicalein treatment significantly decreased the expression of AIF protein in mitochondrial as shown in Fig. 6b. At the same time, we found the levels of DNA repairing enzyme PARP-1 were reduced in OGD group cells. Following baicalein treatment, the amounts of PARP-1 were significantly increased compared to the OGD group. This suggests that the regulation on DNA repairing enzyme is also involved in baicalein-induced cell protection after OGD.

Baicalein has no effect on BAX, Bcl-2, Bcl-XL and cytochrome C expression in OGD treated cells

Furthermore, we investigated some protein related to cell apoptosis to see if they are involved in the protection of OGD cells after baicalein treatment. The anti-apoptotic protein Bcl-2, Bcl-XL and pro-apoptotic protein BAX were measured using Western blot in each group. The data showed that the increased expression of Bcl-2 and Bcl-XL and decreased amounts of BAX in OGD group cells as compared to the control group. However, baicalein didn't cause any changes on these apoptotic proteins. Similarly, the expression of cytochrome C has no significant differences in each group (Fig. 6d).

Baicalein inhibited MIF nuclear translocation in OGD treated cells

MIF translocation and MIF/AIF proteins interaction after OGD were investigated in the cells. Firstly, the protein expression of MIF in nuclear and cytoplasmic fraction was measured by Western blot analysis. As shown in Fig. 7a–d, higher amounts of MIF were translocated into nuclear

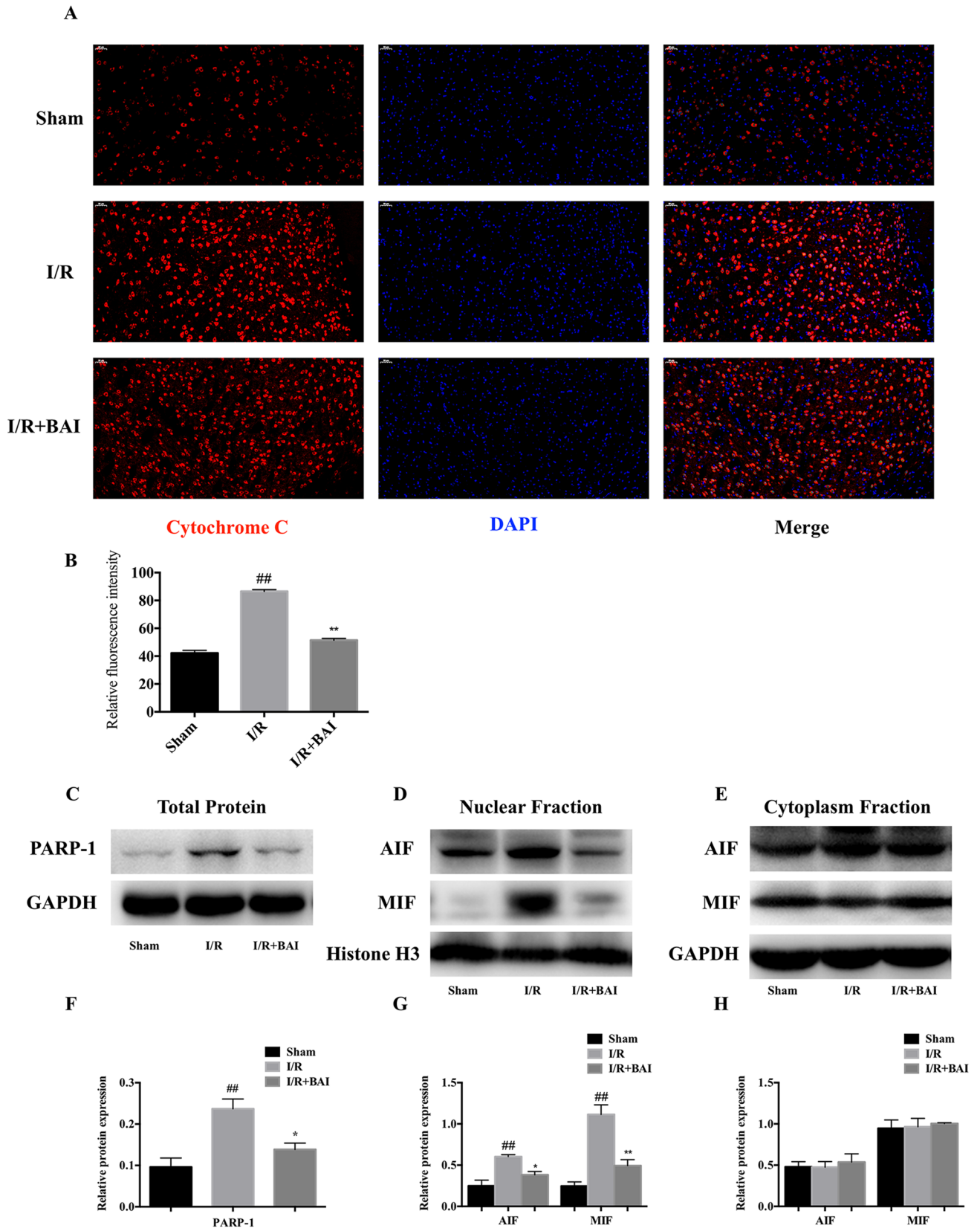


Fig. 3 Effect of baicalein on expression of cytochrome C, PARP-1 and MIF, AIF nuclear translocation in ischemic cortices of cerebral I/R rats. **a** Representative images of cytochrome C expression in cortices of ischemic hemispheres by immunochemical staining. Red stains indicate the cytochrome C protein signal, scale bar = 50 μ m. **b** Statistical analysis of relative fluorescence intensity of cytochrome C in each group. **c** Western blot analysis on PARP-1 protein expression with 3 replicates in each group **d** Representative western blot analysis images of MIF and AIF in nuclear fraction. **e** Representative western blot analysis image of MIF and AIF in cytoplasmic fraction. **f** Statistical analysis of relative protein expression of PARP-1 in each group. **g** Statistical analysis of relative protein expression of AIF, MIF in nuclear fraction of each group. **h** Statistical analysis of relative protein expression of AIF, MIF in cytoplasm fraction of each group. Data were presented as mean \pm SEM (n=03 in each group). ^{##}p < 0.01 vs. sham group; *p < 0.05, **p < 0.01 vs. I/R group

fraction after OGD. In comparison, the amounts of MIF in the nuclear fraction were significantly reduced in baicalein treatment cells. In the following co-immunoprecipitation analysis, the data showed that MIF was well captured by anti-MIF antibody in resin. In control group, no interaction between MIF and AIF was observed. However, an effective co-precipitation between MIF and AIF was detected in OGD and OGD + BAI-5 groups. This suggested that the interaction between MIF and AIF was activated following 12 h OGD exposure, but there were no differences between OGD and baicalein treated OGD group (Fig. 7e).

Discussion

Ischemic stroke is caused by blocking blood supply in brain and the early blood reperfusion can reduce the damage caused by ischemia [2]. However, complex pathological processes can occur due to inflammation and cells death after reperfusion [28, 29]. The studies showed the injury processes evolved at a slow pace and might gradually cause damages to the tissue on the border of the ischemic territory [11, 30]. Therefore, more neuroprotection agents need to be explored to reduce the reperfusion injury after ischemic stroke. The goal of this study is to determine if baicalein treatment can protect brain injury from ischemic stroke and explore its signal transduction mechanisms in MCAO rats and OGD cell models.

The program cells death is a complex process involved in ischemic injury [11]. The ischemic tissue including the core as well as the penumbra, the ischemic penumbra would develop into the core in few days after stroke if there is no pharmacological intervention available [7]. Cytokines were secreted in severe hours after stroke until peaked in few days, which orchestrated cells suicide from penumbra into core [30, 31]. Based on our data obtained from Protein Array analysis, it is noted that the cytokines cascade was

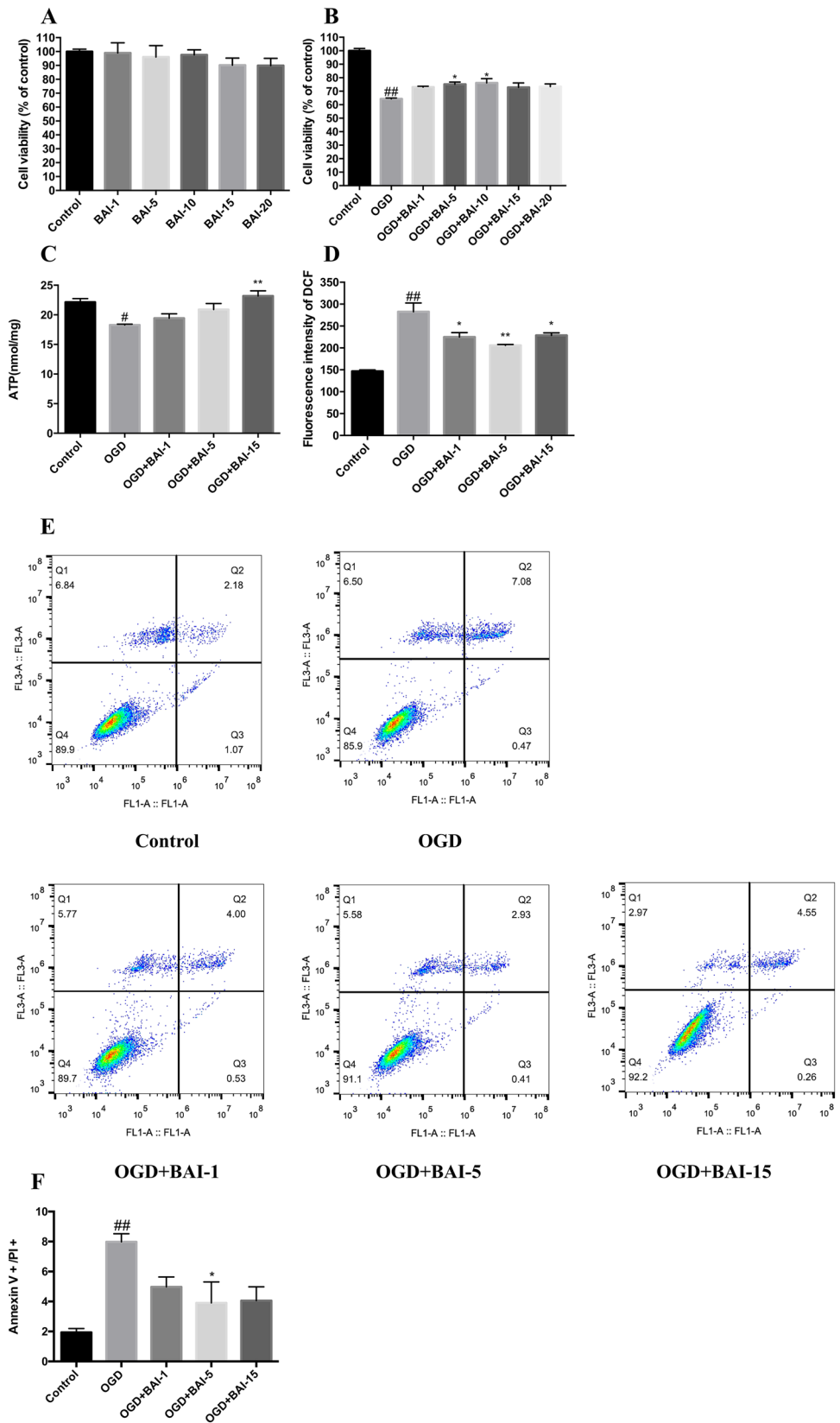
significantly suppressed in baicalein treated group after cerebral I/R. This might be one of mechanisms to reduce infarct volume after baicalein treatment.

Caspase family is a group of cysteine proteases, which is essential for programmed cell death in a variety of species [32, 33]. The published studies have shown that caspase family played an important role in ischemia-mediated cell apoptosis [34, 35]. Some drugs have been developed to suppress apoptosis that is mediated by blocking caspase family member or increasing anti-apoptotic protein expression in mitochondrial of ischemic cells [36–38]. However, the latest studies showed a new form of cell death called pathanatos, which is independent from caspase activation. After ischemic attack, the ROS in mitochondrial caused DNA damage which was detected by PARP-1 and followed by PAR polymers synthesis [18]. Mitochondria housed the death effector AIF, the interaction between AIF and mitochondrial membrane was disrupted by the PAR binding, which led to mitochondrial AIF translocation [18, 39]. Once AIF entered the nucleus, chromatolysis and large-scale DNA degradation happened followed by cells death [17]. AIF itself has no obvious nuclease activity, but it carried an AIF-associated nuclease into the nucleus. Recently, MIF was identified as the nuclease carried into the nucleus by AIF. MIF has rather weak nuclease activity without AIF, knock-down of AIF by RNA interference reduced PAR-dependent cell death [15]. In addition, prevention of the translocation of MIF from cytoplasm to the nucleus by inhibiting mitochondrial AIF nuclear translocation or disrupting AIF and MIF interaction can establish a protection mechanism against ischemic reperfusion injury [15].

In current study our data showed PARP-1 was significantly increased at the day 7 after reperfusion in rats. The baicalein treatment suppressed its expression and subsequently inhibited the nuclear translocation of AIF and MIF molecular. This might explain the neuroprotective mechanism of baicalein treatment in cerebral reperfusion injury of the rats. Additionally, we found that baicalein can inhibit the expression of cytochrome C after cerebral I/R. Since cytochrome C is released from mitochondrial and acts as a trigger for caspase activation, the data suggest that the inhibition of caspase-mediate apoptosis and caspase-independent cells death may both play important roles in the neuroprotection of baicalein treatment in rats with cerebral reperfusion injury [40].

To confirm the mechanisms of neuroprotection following baicalein treatment, we further investigated the detailed caspase-independent signal pathway using in vitro low oxygen and glucose cell culture model. Firstly, it was noted that baicalein can restore the cellular ATP production and mitochondrial potential, inhibit oxidative stress and apoptosis in OGD cells. All these contributed to the protection of cells from ischemic injury after baicalein treatment [41].

Fig. 4 Effect of baicalein on cell viability, mitochondrial function and cell apoptosis and necrosis after OGD. **a** Evaluation of baicalein cytotoxicity on SH-SY5Y cells at the dose of 1–20 μ M. **b** Effects of baicalein treatment on cell viability after OGD in SH-SY5Y cells. **c** Effect of baicalein treatment on ATP levels after OGD. **d** Effect of baicalein treatment on ROS production after OGD in SH-SY5Y cells. **e** Representative scatter diagram of flow cytometry, X-axis was Annexin V signal and Y-axis was PI signal, then the lower left quadrant (Annexin V-/PI-) represents living cells, the lower right quadrant (Annexin V+/PI-) represents early apoptotic cells, the upper right quadrant (Annexin V+/PI+) represents late apoptotic cells and necrotic cells, the upper left quadrant (Annexin V-/PI+) is considered as detection error. **f** Statistical analysis of Annexin V+/PI+ ratio in flow cytometry. Data were presented as mean \pm SEM (n = 03 in each group). ##p < 0.01 vs. sham group; *p < 0.05, **p < 0.01 vs. I/R group



Similar to the results obtained from the cerebral I/R rats, baicalein treatment inhibited the AIF/MIF translocation in nucleus of OGD cells. Interestingly, there was no difference observed in expression of cytochrome C among each group after OGD, which is not consistent with the results obtained from the reperfusion injury group of rats. Also, it is noted that PARP-1 decreased after OGD in cells instead of elevation as observed in rats. This might be due to the large amounts of consumption of this DNA repairing enzyme during acute OGD induced damage. After baicalein treatment, the PARP-1 was returned to the same amounts of control cells. From the flow cytometry, we also found that baicalein reduced the ratio of the apoptotic cells after OGD.

Taken together, our results showed for the first time that the neuroprotection of ischemic tissues and cells by baicalein treatment is regulated through PARP-1 and AIF/MIF signaling pathway. Both in vivo and in vitro models suggested that the inhibition of AIF and MIF nuclear translocation might be the key in the regulation of tissue recovery from ischemic injury after baicalein treatment. The results provided initial evidence that baicalein could be a potential therapeutic candidate to reduce cerebral tissue injury in ischemic stroke, the related proteins might serve as the effective targets for neuroprotective drug development in the future.

Materials and methods

Animals and MCAO model

40 male Sprague-Dawley rats (240–260 g) were purchased from Vital River Laboratory Animal Technology Co. (SCXK (Jing) 2016-0006, Beijing, China). Animals were housed under standard temperature and humidity, diurnal lighting conditions and allowed food and tap water ad libitum. All animal care and experimental procedures were approved by the ethic committees of Institute of Materia Medical, Chinese Academy of Medical Sciences & Peking Union Medical College. The focal cerebral I/R was established as described previously [42]. Briefly, after acclimation for 3 days, the rats were anesthetized by the intraperitoneal injection of sodium pentobarbital (30 mg/kg). Heating pad was used to maintain a rectal temperature of 37.0 ± 0.5 °C during the study. The right common carotid artery (cca.), external carotid artery (ECA) and internal carotid artery (ICA) were isolated. Then, the standardized nylon suture was inserted from the ECA into the ICA until the marker on suture shown on the intersection of ECA and ICA, which indicated that the suture successfully blocked the middle cerebral artery (MCA). Regional cerebral blood flow was monitored using Laser Doppler Flowmetry (LDF) (PeriFlux 5000, PERIMED, Sweden). It showed that the ligation reduced blood flow to 20% of the baseline during MCAO. After 60 min MCAO, nylon

suture was removed to start reperfusion, LDF showed blood flow returned to 100% of the baseline in all animals. The rats were randomly divided into 3 groups: Sham group (Sham), cerebral I/R group (I/R), cerebral I/R treated with 100 mg/kg baicalein group (I/R + BAI). Rats in the sham operation group underwent the same procedure without occlusion of the MCA. The mortality of the rats in ischemic groups was 14.3% (4/28) due to brain damage. All the rats in the sham group were survived.

Baicalein (purity > 98%) was provided by Prof. Lyu Yang of the Institute of Materia Medica, Chinese Academy of Medical Sciences and Peking Union Medical College. It was prepared in saline containing 0.5% sodium carboxymethylcellulose (CMC-Na) and delivered by intragastric at oral dose of 100 mg/kg daily for 7 days. The rats in the sham group and I/R group were treated with the vehicle (0.5% CMC-Na in saline) in the same manner. Drug and vehicle were administered blindly.

Neurological examination and TTC staining

To examine the stroke injury on the brain of each rat, evaluation on cerebral ischemic damage including neurological examination and TTC staining to measure infarct volume on day 7. A neurological examination was performed on each rat before termination. Neurologic score was derived using a 5-point scale as described in the published study [42]: 0, no neurological deficits; 1, cannot extend left forelimb fully; 2, cannot walk straightly; 3, circle to the left; 4, inability to walk spontaneously or losing consciousness.

After neurological examination, the rats were sacrificed and the infarct volume of brain was examined using TTC staining. The brain tissues were dissected coronally into 2-mm slices using a scalpel. The sections were stained by 1% 2,3,5-tripenyltetrazolium chloride (TTC, Sigma, St. Louis, MO, USA) at 37 °C for 30 min, and then fixed in 4% paraformaldehyde at room temperature overnight prior to imaging. The infarct area in each section was evaluated using the Image J/Fiji processing system [43]. The percentage of the infarct volume was calculated using the following formula. The sum of infarct area/the sum of sections area $\times 100\%$.

Magnetic resonance imaging

On day 1, day 4 and day 7 after MCAO surgery, cerebral infarction and edema of each rat were evaluated using MRI (Bruker PharmaScan 7.0 T/16 US system, Germany) after anesthetized with isoflurane. Five scanned sections with each 1 mm thickness were obtained. In the scanned sections, the grey region represents the viable tissues and the white region indicates the infarct tissue. The following formula was used

A

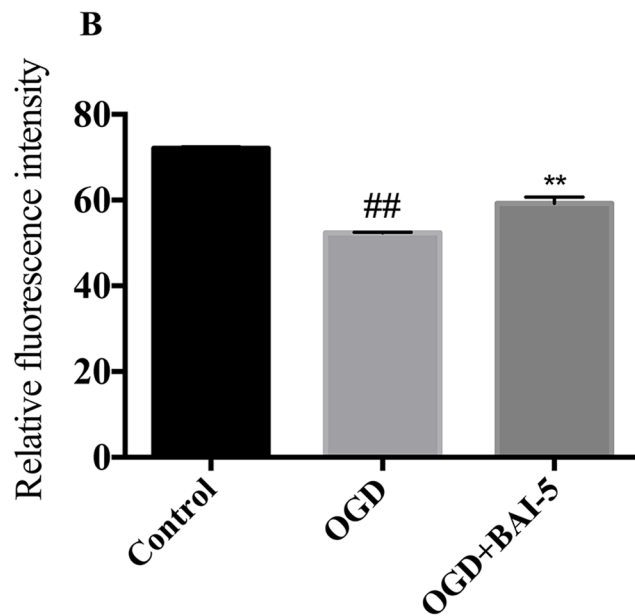
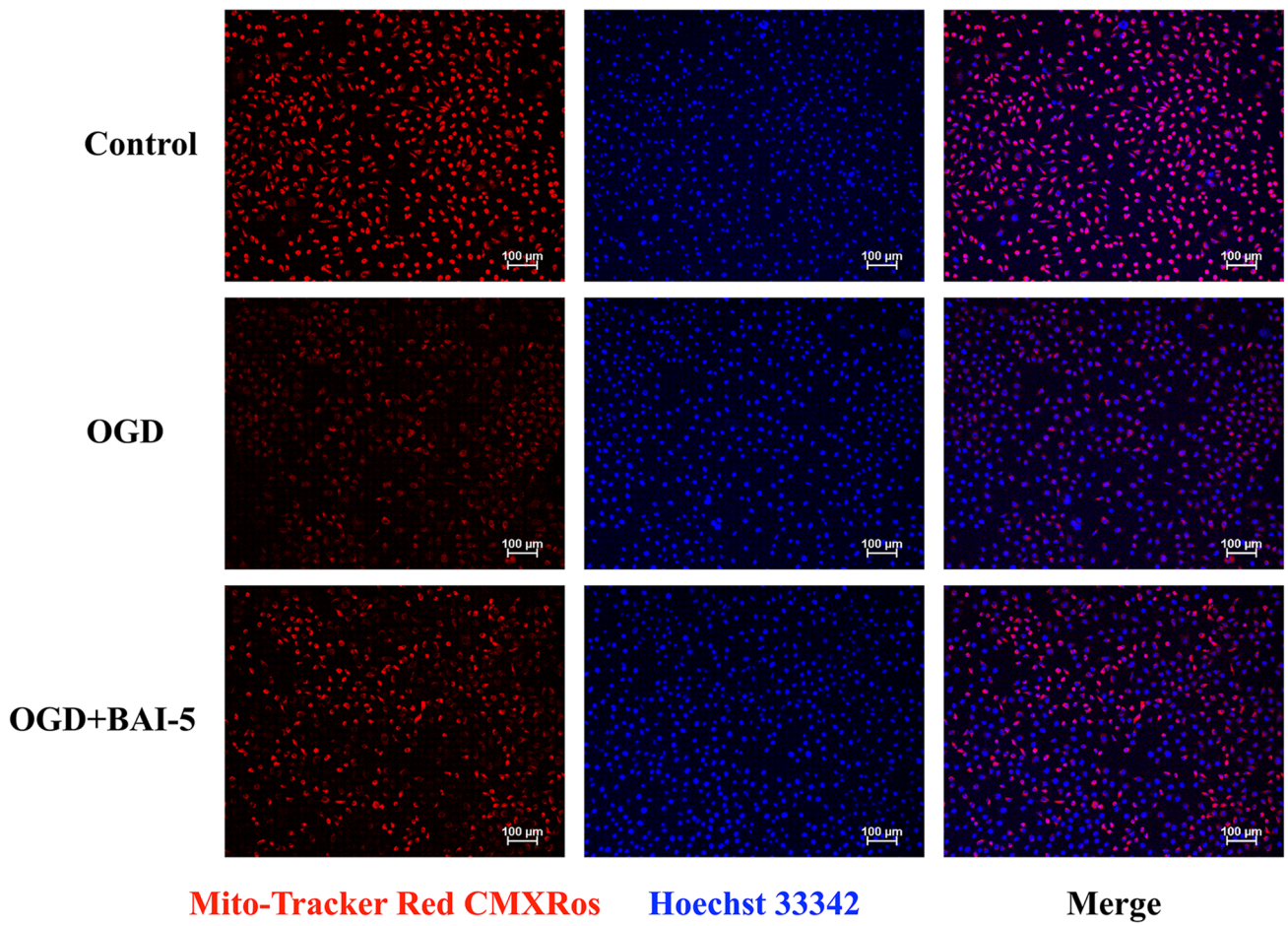


Fig. 5 Effects of baicalein on intracellular mitochondrial membrane potential in SH-SY5Y cells. **a** Representative images of Mito-Tracker Red CMXRos positive staining on mitochondrial membrane potentials. **b** Statistical analysis of relative fluorescence intensity of mitochondrial membrane potential using Mito-Tracker Red CMXRos dye. The nuclear was stained as blue with Hoechst 33342 dye. Data were presented as mean \pm SEM (n=03 in each group). $^{###}p < 0.01$ vs. sham group; $^{*}p < 0.05$, $^{**}p < 0.01$ vs. I/R group

to calculate the infarct volume and edema ratio in each rat: Infarct volume = (The sum of infarct area/the sum of scanned sections area) \times 100%.

Edema ratio = [(The sum of ischemic hemisphere area – the sum of other hemisphere area)/the sum of scanned sections area] \times 100%.

Cytokine analysis

The proteins of ischemic cortices were collected and its total amounts were determined by BCA protein assay kit (Thermo, Rockford, USA). Then the Protein Array Assay (Cat#: QAR-CAA-67, RayBiotech, Norcross, GA) was conducted according to the manufacturer's instructions. Firstly, each protein chip was blocked with blocking buffer for 30 min. Then the blocking buffer was removed and 50 μ g protein samples was added to each well. The chips were incubated overnight at 4 °C. After washing, each chip was incubated with biotinylated antibody for 2 h, and Cy3 Equivalent Dye Streptavidin for 1 h, respectively. After washing, the fluorescence was measured at wave length of 532 nm using InnoScan 300 Microarray Scanner (Innopsys, France).

Immunofluorescence detection of cytochrome C

At necropsy, rats were anesthetized and perfused intracardially with PBS and then with 4% paraformaldehyde (PFA). The brain tissues were fixed in 4% PFA overnight at 4 °C. The tissues were sectioned with 20 μ m thickness using a rotary microtome (RM2016, Leica, Germany) by paraffin section method. The immunofluorescence was performed on paraffin sections. Firstly, dewax paraffin section to water and repair antigen in citric acid antigen repair buffer. Then blocked by 2% BSA at room temperature for 30 min. The BSA was incubated with cytochrome C primary antibody (1:200) at 4 °C overnight and then detected using secondary goat anti-rabbit antibodies (Wuhan Servicebio technology, China) for 50 min at room temperature. After washing with PBS for three times, the section was incubated with CY3 (Servicebio technology) for 10 min and then washed with TBST. The fluorescent quencher was added to the slice for 5 min incubation. After washing, cell nuclei were stained with DAPI (Servicebio technology) for 10 min. All images were acquired using fluorescence microscope (Eclipse C1, Nikon, Japan). Fluorescence intensity was analyzed using the image

processing software Image J/Fiji [43]. Cortices of ischemic hemispheres were selected for analysis (3 rats in each group and 3 slides per rat).

Cell culture and viability assay

Human neuroblastoma SH-SY5Y cells purchased from Institute of Basic Medical Sciences, Chinese Academy of Medical Sciences & Peking Union Medical College (Beijing, China) were maintained in DMEM medium supplemented with 10% FBS (Invitrogen) plus 1% penicillin/streptomycin (Invitrogen) in the incubator at 37 °C with 5% CO₂/95% air. Baicalein was dissolved in DMSO to prepared 100 mM baicalein reserved solution and then dilute into 1, 5, 10, 15, 20 μ M with saline for treatment.

Cell viability was determined using CCK-8 assay. Briefly, the SH-SY5Y cells were seeded into 96-well plates at a density of 5×10^3 cells/well. After 24 h, cells were treated with baicalein at the dose of 0, 1, 5, 10, 15, 20 μ M and OGD was induced by exposing cells to glucose and serum free DMEM medium with 1% O₂ in O₂/N₂/CO₂ incubator (ASTEC SMA-30D, Japan) for 12 h. The cells in control group were treated with the saline and incubated with 5% CO₂/95% air in the incubator. After incubation, 10 μ L CCK-8 reagent were added into each well and incubated with cells for 2 h. Absorbance was detected at the wavelength of 450 nm and used to calculate the cell viability according to the manufacturer's instructions.

Measurement of ATP

The ATP production was measured by Firefly Luciferase Method using an enhanced ATP Assay Kit (Beyotime, Shanghai, China). Cells were seeded into 6-well plates at a density of 1×10^6 cells/well and OGD was induced in the same manner as we mentioned above. After 12 h OGD, cells were collected for ATP measurement according to the manufacturer's instructions. The concentration of ATP was normalized by the total amount of protein as measured from the cells.

Measurement of reactive oxygen species (ROS)

Ischemia injury caused accumulation of ROS and followed by DNA damage, PARP-1 activation. Thus, the ROS production was measured using fluorescent probe DCFH-DA with ROS Assay Kit (Beyotime, Shanghai, China). Briefly, the cells were seeded into 96-well plates at a density of 5×10^3 cells/well and OGD was induced in the same manner as we mentioned above. After 12 h OGD, the culture medium was removed and 10 μ M DCFH-DA was added to the cells.

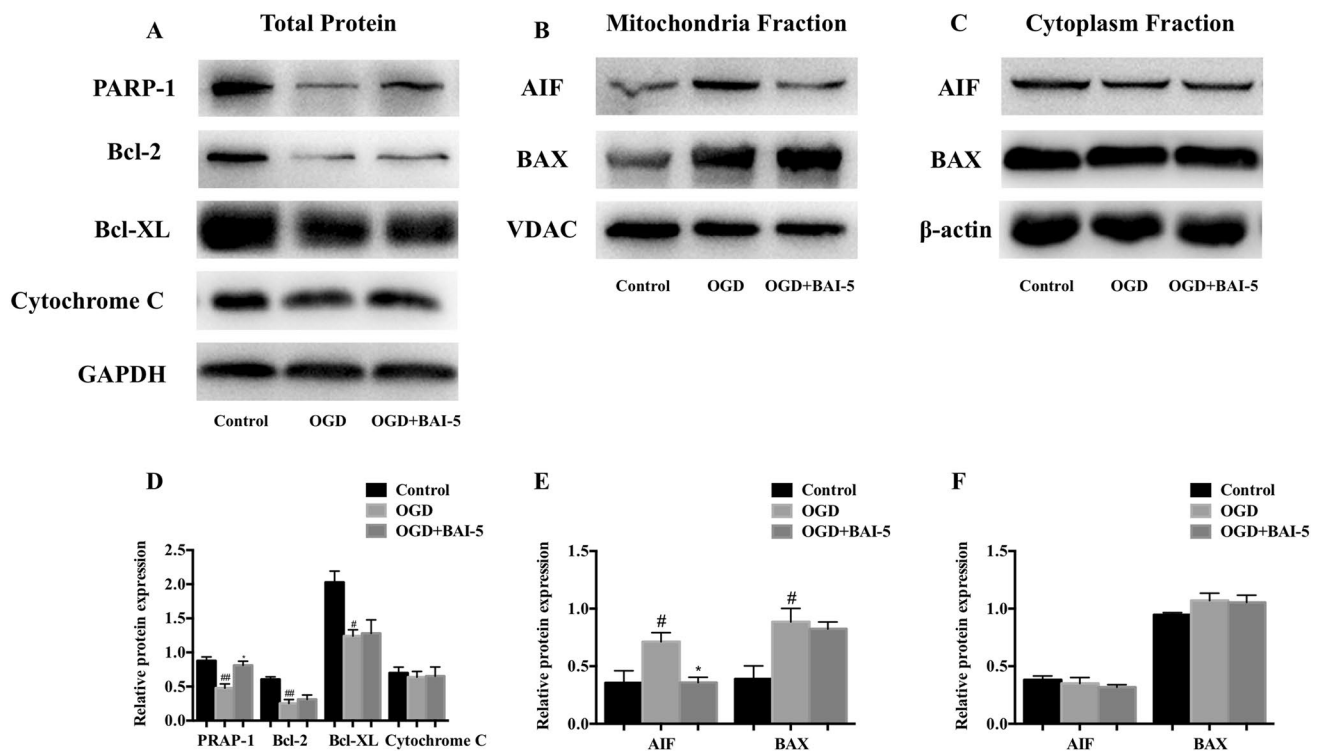


Fig. 6 Effects of baicalein on expression of PARP-1, Bcl-2, Bcl-XL, cytochrome C and AIF, BAX mitochondria translocation in SH-SY5Y cells. **a** Representative Western blot images of total PARP-1, Bcl-2, Bcl-XL, cytochrome C protein expression in each group. **b** Representative Western blot images of AIF and BAX expression in mitochondria fraction in each group. **c** Representative Western blot images of AIF and BAX expression in cytoplasmic fraction in each

group. **d** Quantitative analysis of protein expression of PARP-1, Bcl-2, Bcl-XL, cytochrome C in each group. **e** Quantitative analysis of protein expression of AIF and BAX in mitochondria fraction in each group. **f** Quantitative analysis of protein expression of AIF, BAX in cytoplasmic fraction in each group. Data were presented as mean \pm SEM ($n=03$ in each group). $##p<0.01$ vs. sham group; $*p<0.05$, $**p<0.01$ vs. I/R group

After 20 min incubation at 37°C, the cells were washed with serum free medium for 3 times. The fluorescence intensity was determined at excitation wavelength 488 nm and emission wavelength 525 nm using a spectrophotometer.

Flow cytometry analysis

The apoptosis and necrosis of SY5Y cells were stained with TransDetect Annexin V-FITC/PI Cell Apoptosis Detection Kit (Transgene, Beijing, China) by flow cytometry detection. Cells were seeded into Petri dish at a density of 1×10^6 cells/well and OGD was introduced in the same manner as we mentioned above. After 12 h OGD, cells were collected with EDTA free pancreatin, centrifuged at 500 g at 4°C for 5 min and washed twice with cold PBS. After adding 100 μ L cold Annexin V Binding Buffer, cells were resuspended. Then 5 μ L Annexin V-FITC and 5 μ L PI were added and the cells were incubated in dark at 25°C for 15 min. Following

adding 400 μ L cold Annexin V Binding Buffer, the cells were resuspended and stained for flow cytometry analysis.

Fluorescence detection of mitochondrial membrane potential

The cells mitochondrial membrane potential was detected by Mito-Tracker Red CMXRos (Beyotime, Shanghai, China), which is specifically binding to bioactive mitochondrial and detect the membrane potential. Cells were seeded into 96-well plates at a density of 5×10^3 cells/well and OGD was introduced in the same manner as we mentioned above. After 12 h OGD, the 96-well plate was centrifuged at 1000 g for 5 min. The culture medium was removed and Mito-Tracker Red CMXRos and Hoechst 33342 were added to the cells. After 30 min incubation in the dark at 25°C, the images were taken using fluorescence microscope. The fluorescence intensity was analyzed using the image processing software J/Fiji.

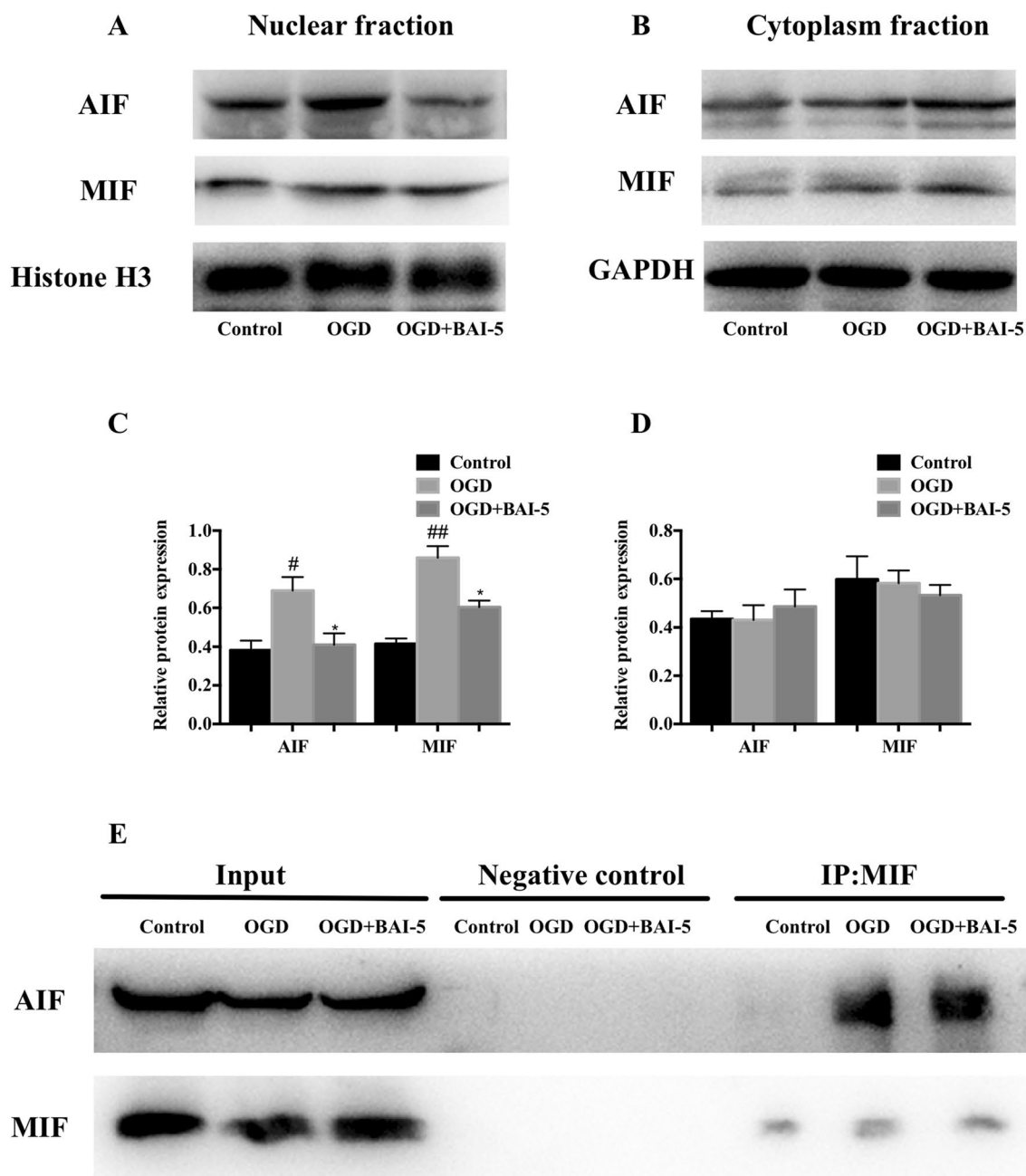


Fig. 7 Effect of baicalein on AIF, MIF nuclear translocation and AIF/MIF interaction in SH-SY5Y cells. **a** Representative Western blot images of AIF and MIF protein expression in nuclear fraction of each group. **b** Representative Western blot images of AIF and MIF protein expression in cytoplasmic fraction of each group. **c** Quantitative analysis of AIF and MIF protein expression in nuclear fraction of

each group. **d** Quantitative analysis of AIF and MIF protein expression in cytoplasmic fraction of each group. **e** Representative Western blot image by co-immunoprecipitation analysis. Data were presented as mean \pm SEM ($n=03$ in each group). $^{##}p<0.01$ vs. sham group; $^{*}p<0.05$, $^{**}p<0.01$ vs. I/R group

Co-immunoprecipitation (CO-IP)

To investigate the interaction between AIF and MIF in SH-SY5Y cells, we conducted Co-immunoprecipitation experiment using Pierce CO-IP kit (Thermo Fisher Scientific

Inc, USA). Proteins were collected as described in Western blot, and the concentration of each protein was normalized by the total amount of protein as measured from BCA assay. Anti-MIF antibody (ab175189, 1:1000) was immobilized onto AminoLink coupling resin, the rabbit

anti-Mouse IgG (Applygen Technologies Inc, Beijing, China) was immobilized to resin in same manner as negative controls. After washing, 500 μ L sample was added to each resin and incubated overnight at 4°C. After incubation, the resin was washed 3 times with IP lysis/washing buffer and eluted with elution buffer for 5 min. Then the elution was centrifuged and collected to measure the MIF and AIF by Western blot.

Isolation of proteins and Western blot analysis

The cortices of ischemic hemisphere and the cultured SH-SY5Y cells were collected to examine the protein expression of PARP-1, AIF, MIF, Bcl-2, Bcl-XL, cytochrome C, BAX. The nuclear fraction was extracted with nuclear-cytosol extraction kit (Applygen Technologies Inc, Beijing, China), mitochondrial fraction was extracted with mitochondria isolation kit (Applygen Technologies Inc, Beijing, China). Cells or brain tissues were mixed with RIPA buffer including cocktail protease inhibitor (100 mg/mL). Proteins were separated by sodium dodecyl sulfate-polyacrylamide gel electrophoresis (SDS-PAGE) and transferred to PVDF membrane for Western blot analysis. The following primary antibodies were used to detect the proteins: anti-PARP-1 antibody (ab227244, 1:1000), anti-MIF antibody (ab175189, 1:1000), anti-AIF antibody (ab32516, 1:1000), anti-Bcl-2 antibody (CST#15071, 1:1000), anti-Bcl-XL antibody (CST#2764, 1:1000), anti-Cytochrome C antibody (ab133504, 1:1000), anti-GAPDH antibody (ab181602, 1:1000), anti-Histone H3 antibody (CST#4499, 1:1000), anti-VDAC antibody (ab15895, 1:1000), anti-BAX antibody (CST#5023, 1:1000), anti- β -actin antibody (C1313, 1:1000). The membranes were incubated with secondary antibody for 2 h at room temperature. The protein expression was detected using enhanced ECL system. Optical density values of each detected protein were analyzed using the ImageJ/Fiji processing system. GAPDH, β -actin, Histone H3, VDAC were used as reference control to normalize the detected proteins.

Statistical analysis

The differences between each group was analyzed using GraphPad Prism software (version 7.04). Data were presented as mean \pm SEM. One-way ANOVA was used to calculate differences between the various groups. Tukey's multiple comparison post hoc test was performed to determine significance levels. Statistical significance was considered at $p < 0.05$.

Author contributions W-HL, Y-LY, XC, ML, and S-SZ performed the animal experiments; W-HL analyzed the data and wrote the

manuscript; Y-HW and G-HD designed the experiments and revised the manuscript; and all authors read and approved the final manuscript.

Funding This project was supported by the National Key Research & Development Plan (2018YFC0311005), the Significant New-Drugs Creation of Science and Technology Major Projects (2018ZX09711001-003-019), the National Natural Science Foundation of China (81473383), the Medical and Health Innovation Project of Chinese Academy of Medical Sciences (2016-I2M-3-007), and Innovation Fund for Doctoral Students of Beijing Union Medical College (2018-1007-04).

Compliance with ethical standards

Conflict of interest All authors declare that they have no competing interests.

References

- Mendy VL, Vargas R, Payton M, Sims JN, Zhang L (2019) Trends in the stroke death rate among Mississippi adults, 2000–2016. *Prev Chronic Dis* 16:E21–E21. <https://doi.org/10.5888/pcd16.180425>
- Hankey GJ (2017) Stroke. *Lancet* 389(10069):641–654. doi:[https://doi.org/10.1016/S0140-6736\(16\)30962-X](https://doi.org/10.1016/S0140-6736(16)30962-X)
- McDermott M, Skolarus LE, Burke JF (2019) A systematic review and meta-analysis of interventions to increase stroke thrombolysis. *BMC Neurol* 19(1):86–86. doi:<https://doi.org/10.1186/s12883-019-1298-2>
- Jovin TG (2018) MRI-guided intravenous alteplase for stroke - still stuck in time. *N Engl J Med* 379(7):682–683. <https://doi.org/10.1056/NEJMe1805796>
- Halder SK, Matsunaga H, Ueda H (2019) Prothymosin alpha and its mimetic hexapeptide improve delayed tissue plasminogen activator-induced brain damage following cerebral ischemia. *J Neurochem*. doi:<https://doi.org/10.1111/jnc.14858>
- Abdelmalik PA, Ziai WC (2017) Spontaneous intraventricular hemorrhage: when should intraventricular tPA be considered? *Semin Respir Crit Care Med* 38(6):745–759. <https://doi.org/10.1055/s-0037-1607991>
- Venkat P, Shen Y, Chopp M, Chen J (2018) Cell-based and pharmacological neurorestorative therapies for ischemic stroke. *Neuropharmacology* 134(Pt B):310–322. <https://doi.org/10.1016/j.neuropharm.2017.08.036>
- Amani H, Habibey R, Shokri F, Hajmiresmail SJ, Akhavan O, Mashaghi A, Pazoki-Toroudi H (2019) Selenium nanoparticles for targeted stroke therapy through modulation of inflammatory and metabolic signaling. *Sci Rep* 9(1):6044. doi:<https://doi.org/10.1038/s41598-019-42633-9>
- Amani H, Mostafavi E, Alebouyeh MR, Arzaghi H, Akbarzadeh A, Pazoki-Toroudi H, Webster TJ (2019) Would colloidal gold nanocarriers present an effective diagnosis or treatment for ischemic stroke? *Int J Nanomed* 14:8013–8031. <https://doi.org/10.2147/IJN.S210035>
- Jun-Long H, Yi L, Bao-Lian Z, Jia-Si L, Ning Z, Zhou-Heng Y, Xue-Jun S, Wen-Wu L (2018) Necroptosis signaling pathways in stroke: from mechanisms to therapies. *Curr Neuropharmacol* 16(9):1327–1339. <https://doi.org/10.2174/1570159X16666180416152243>
- Uzdensky AB (2019) Apoptosis regulation in the penumbra after ischemic stroke: expression of pro- and antiapoptotic proteins.

- Apoptosis 24(9–10):687–702. doi:<https://doi.org/10.1007/s10495-019-01556-6>
12. Gong L, Tang Y, An R, Lin M, Chen L, Du J (2017) RTN1-C mediates cerebral ischemia/reperfusion injury via ER stress and mitochondria-associated apoptosis pathways. *Cell Death Dis* 8(10):e3080. doi:<https://doi.org/10.1038/cddis.2017.465>
 13. Stockwell BR, Friedmann Angeli JP, Bayir H, Bush AI, Conrad M, Dixon SJ, Fulda S, Gascón S, Hatzios SK, Kagan VE, Noel K, Jiang X, Linkermann A, Murphy ME, Overholtzer M, Oyagi A, Pagnussat GC, Park J, Ran Q, Rosenfeld CS, Salnikow K, Tang D, Torti FM, Torti SV, Toyokuni S, Woerpel KA, Zhang DD (2017) Ferroptosis: a regulated cell death nexus linking metabolism, redox biology, and disease. *Cell* 171(2):273–285. <https://doi.org/10.1016/j.cell.2017.09.021>
 14. Arumugam TV, Baik S-H, Balaganapathy P, Sobey CG, Mattson MP, Jo D-G (2018) Notch signaling and neuronal death in stroke. *Prog Neurobiol* 165–167:103–116. doi:<https://doi.org/10.1016/j.pneurobio.2018.03.002>
 15. Wang Y, An R, Umanah GK, Park H, Nambiar K, Eacker SM, Kim B, Bao L, Harraz MM, Chang C, Chen R, Wang JE, Kam TI, Jeong JS, Xie Z, Neifert S, Qian J, Andrabi SA, Blackshaw S, Zhu H, Song H, Ming GL, Dawson VL, Dawson TM (2016) A nuclease that mediates cell death induced by DNA damage and poly(ADP-ribose) polymerase-1. *Science*. <https://doi.org/10.1126/science.aad6872>
 16. Zhang R, Tang S, Huang W, Liu X, Li G, Chi H, Zhu M, Tang J (2015) Protection of the brain following cerebral ischemia through the attenuation of PARP-1-induced neurovascular unit damage in rats. *Brain Res* 1624:9–18. <https://doi.org/10.1016/j.brainres.2015.07.023>
 17. Raghavan A, Shah ZA (2015) Withania somnifera improves ischemic stroke outcomes by attenuating PARP1-AIF-mediated caspase-independent apoptosis. *Mol Neurobiol* 52(3):1093–1105. <https://doi.org/10.1007/s12035-014-8907-2>
 18. Dawson TM, Dawson VL (2017) Mitochondrial mechanisms of neuronal cell death: potential therapeutics. *Annu Rev Pharmacol Toxicol* 57:437–454. <https://doi.org/10.1146/annurev-pharmtox-010716-105001>
 19. Sies H, Berndt C, Jones DP (2017) Oxidative stress. *Annu Rev Biochem* 86:715–748. <https://doi.org/10.1146/annurev-biochem-061516-045037>
 20. Kim Y, Kim YS, Kim HY, Noh MY, Kim JY, Lee YJ, Kim J, Park J, Kim SH (2018) Early treatment with Poly(ADP-Ribose) polymerase-1 inhibitor (JPI-289) reduces infarct volume and improves long-term behavior in an animal model of ischemic stroke. *Mol Neurobiol* 55(9):7153–7163. <https://doi.org/10.1007/s12035-018-0910-6>
 21. Noh MY, Lee WM, Lee SJ, Kim HY, Kim SH, Kim YS (2018) Regulatory T cells increase after treatment with poly (ADP-ribose) polymerase-1 inhibitor in ischemic stroke patients. *Int Immunopharmacol* 60:104–110. doi:<https://doi.org/10.1016/j.intimp.2018.04.043>
 22. Leprêtre C, Tchakarska G, Blibech H, Lebon C, Torriglia A (2013) Apoptosis-inducing factor (AIF) and leukocyte elastase inhibitor/L-DNase II (LEI/LDNaseII), can interact to conduct caspase-independent cell death. *Apoptosis* 18(9):1048–1059. <https://doi.org/10.1007/s10495-013-0862-2>
 23. Yang S, Wang H, Yang Y, Wang R, Wang Y, Wu C, Du G (2019) Baicalein administered in the subacute phase ameliorates ischemia-reperfusion-induced brain injury by reducing neuroinflammation and neuronal damage. *Biomed Pharmacother* 117:109102. doi:<https://doi.org/10.1016/j.biopha.2019.109102>
 24. Liang W, Huang X, Chen W (2017) The effects of baicalin and baicalein on cerebral ischemia: a review. *Aging Dis* 8(6):850–867. <https://doi.org/10.14336/AD.2017.0829>
 25. Liu C, Wu J, Xu K, Cai F, Gu J, Ma L, Chen J (2010) Neuroprotection by baicalein in ischemic brain injury involves PTEN/AKT pathway. *J Neurochem* 112(6):1500–1512. doi:<https://doi.org/10.1111/j.1471-4159.2009.06561.x>
 26. Cui L, Zhang X, Yang R, Liu L, Wang L, Li M, Du W (2010) Baicalein is neuroprotective in rat MCAO model: role of 12/15-lipoxygenase, mitogen-activated protein kinase and cytosolic phospholipase A2. *Pharmacol Biochem Behav* 96(4):469–475. <https://doi.org/10.1016/j.pbb.2010.07.007>
 27. Crowley LC, Marfell BJ, Scott AP, Waterhouse NJ (2016) Quantitation of apoptosis and necrosis by annexin V binding, propidium iodide uptake, and flow cytometry. *Cold Spring Harb Protoc* 2016. <https://doi.org/10.1101/pdb.prot087288>
 28. Jin R, Yang G, Li G (2010) Inflammatory mechanisms in ischemic stroke: role of inflammatory cells. *J Leukoc Biol* 87(5):779–789. doi:<https://doi.org/10.1189/jlb.1109766>
 29. Guzik A, Bushnell C (2017) Stroke epidemiology and risk factor management. *Continuum* 23(1):15–39. <https://doi.org/10.1212/CON.0000000000000416>
 30. Ulrich D, Iadecola C, Moskowitz MA (1999) Pathobiology of ischaemic stroke: an integrated view. *Trends Neurosci* 22:391–397
 31. Jin R, Liu L, Zhang S, Nanda A, Li G (2013) Role of inflammation and its mediators in acute ischemic stroke. *J Cardiovasc Transl Res* 6(5):834–851. doi:<https://doi.org/10.1007/s12265-013-9508-6>
 32. Andreas S, O'Connor L, Dixit VM (2000) Apoptosis signaling. *Annu Rev Biochem* 69:217–245
 33. de la GarcíaCadena S, Massieu L (2016) Caspases and their role in inflammation and ischemic neuronal death. *Focus on caspase-12*. *Apoptosis* 21(7):763–777. <https://doi.org/10.1007/s10495-016-1247-0>
 34. Radak D, Katsiki N, Resanovic I, Jovanovic A, Sudar-Milovanovic E, Zafirovic S, Mousad SA, Isenovic ER (2017) Apoptosis and acute brain ischemia in ischemic stroke. *Curr Vasc Pharmacol* 15(2):115–122. <https://doi.org/10.2174/1570161115666161104095522>
 35. Dojo Soeandy C, Salmasi F, Latif M, Elia AJ, Suo NJ, Henderson JT (2019) Endothelin-1-mediated cerebral ischemia in mice: early cellular events and the role of caspase-3. *Apoptosis* 24(7–8):578–595. <https://doi.org/10.1007/s10495-019-01541-z>
 36. Shabanzadeh AP, D'Onofrio PM, Monnier PP, Koeberle PD (2015) Targeting caspase-6 and caspase-8 to promote neuronal survival following ischemic stroke. *Cell Death Dis* 6(11):e1967–e1967. <https://doi.org/10.1038/cddis.2015.272>
 37. Lee H, Shin EA, Lee JH, Ahn D, Kim CG, Kim J-H, Kim S-H (2018) Caspase inhibitors: a review of recently patented compounds (2013–2015). *Expert Opin Ther Pat* 28(1):47–59. doi:<https://doi.org/10.1080/13543776.2017.1378426>
 38. Ha YM, Kim MY, Park MK, Lee YS, Kim YM, Kim HJ, Lee JH, Chang KC (2012) Higenamine reduces HMGB1 during hypoxia-induced brain injury by induction of heme oxygenase-1 through PI3K/Akt/Nrf-2 signal pathways. *Apoptosis* 17(5):463–474. <https://doi.org/10.1007/s10495-011-0688-8>
 39. Pallast S, Arai K, Pekcec A, Yigitkanli K, Yu Z, Wang X, Lo EH, van Leyen K (2010) Increased nuclear apoptosis-inducing factor after transient focal ischemia: a 12/15-lipoxygenase-dependent organelle damage pathway. *J Cereb Blood Flow Metab* 30(6):1157–1167. doi:<https://doi.org/10.1038/jcbfm.2009.281>
 40. Xie Y-L, Zhang B, Jing L (2018) MiR-125b blocks Bax/Cytochrome C/Caspase-3 apoptotic signaling pathway in rat models of cerebral ischemia-reperfusion injury by targeting p53. *Neuro Res* 40(10):828–837. doi:<https://doi.org/10.1080/01616412.2018.1488654>
 41. Szeto V, Chen N-H, Sun H-S, Feng Z-P (2018) The role of K(ATP) channels in cerebral ischemic stroke and diabetes. *Acta Pharmacol Sin* 39(5):683–694. <https://doi.org/10.1038/aps.2018.10>

42. Li WH, Cheng X, Yang YL, Liu M, Zhang SS, Wang YH, Du GH (2019) Kaempferol attenuates neuroinflammation and blood brain barrier dysfunction to improve neurological deficits in cerebral ischemia/reperfusion rats. *Brain Res* 1722:146361. doi:<https://doi.org/10.1016/j.brainres.2019.146361>
43. Schindelin J, Arganda-Carreras I, Frise E, Kaynig V, Longair M, Pietzsch T, Preibisch S, Rueden C, Saalfeld S, Schmid B, Tinevez J-Y, White DJ, Hartenstein V, Eliceiri K, Tomancak P, Cardona A

(2012) Fiji: an open-source platform for biological-image analysis. *Nat Methods* 9(7):676–682. <https://doi.org/10.1038/nmeth.2019>

Publisher's Note Springer Nature remains neutral with regard to jurisdictional claims in published maps and institutional affiliations.